

Measurements of Turbulent Flow and Ozone at Rooftop and Sidewalk Sites in a High-Rise Building Area

Seung-Bu Park¹, Kyung-Hwan Kwak¹, Beom-Soon Han¹, Gantuya Ganbat¹,
Hyunho Lee¹, Jaemyeong Mango Seo¹, Sang-Hyun Lee², and Jong-Jin Baik¹

¹*School of Earth and Environmental Sciences, Seoul National University, Seoul, Republic of Korea*

²*Department of Atmospheric Science, Kongju National University, Gongju, Republic of Korea*

Abstract

Turbulent flow and ozone concentration at two (rooftop and sidewalk) sites in a high-rise building area of Seoul, Republic of Korea, were measured for the period of 24–27 June 2013 to examine their characteristics according to site location. During the observation period, the diurnal variations of air temperature, wind speed, and turbulent kinetic energy were distinct at both sites. The time series of ozone concentration exhibits a diurnal variation with daytime double peaks and one nighttime peak at both sites. The horizontal wind direction at the rooftop site has variations related to local winds, while the horizontal wind direction at the sidewalk site is mostly southerly (following a nearby street). The multiresolution spectra of horizontal and vertical velocities at the rooftop site confirm diurnal and turbulence-related variations. A quadrant analysis indicates that turbulence at the rooftop site is characterized by frequent ejections and less frequent but stronger sweeps, while turbulence at the sidewalk site is weaker and less characterizable than turbulence at the rooftop site.

(Citation: Park, S.-B., K.-H. Kwak, B.-S. Han, G. Ganbat, H. Lee, J. M. Seo, S.-H. Lee, and J.-J. Baik, 2015: Measurements of turbulent flow and ozone at rooftop and sidewalk sites in a high-rise building area. *SOLA*, **11**, 1–4, doi:10.2151/sola.2015-001.)

1. Introduction

Flow/wind in densely built-up urban areas is quite complex. To better understand its complex nature, wind-tunnel or water-channel experimental studies (e.g., Kastner-Klein et al. 2001; Princevac et al. 2010), numerical modeling studies (Letzel et al. 2012; Park et al. 2013), and field experimental studies (e.g., Brown et al. 2004; Zajic et al. 2011) have been performed extensively.

Many researchers have investigated the characteristics of turbulent flow in urban areas (Roth and Oke 1993; Rotach 1995; Nelson et al. 2007, 2011). Louka et al. (2000) showed that turbulent fluctuations comprise a large portion of flow in a street canyon. Dispersion of pollutants in urban areas is strongly influenced by characteristic flow patterns (Allwine et al. 2002; Wood et al. 2009). However, the characterization of urban turbulent flow and dispersion particularly in densely built-up urban areas is still difficult because of their strong dependency on nearby building configurations as well as local meteorology. To further advance our understanding of urban turbulent flow and dispersion, well-purposed field experiments that focus on spatial inhomogeneity and local meteorology are needed.

This study examines the characteristics of turbulent flow and ozone concentration measured at rooftop and sidewalk sites in a high-rise building area of a megacity, focusing on their similarities and differences according to site location. The field experimental setup is described in Section 2, and measurement results are presented and discussed in Section 3. A summary and conclusions are given in Section 4.

2. Field experimental setup

2.1 Measurement sites and weather synopsis

A field experiment was conducted at a central business district, Gangnam, Seoul, Republic of Korea, for 4 consecutive days from 24 to 27 June 2013 (Fig. 1). Two nearby measurement sites are located at the rooftop level of an 8-story building (location A) and the pedestrian level on a sidewalk along Nonhyun Street (NNW–SSE directed with 7 lanes) (location B). A 45-story building, with a height of 206 m, is located to the west of the 8-story building and across Nonhyun Street. Another tall building, with a height of 167 m, is located to the north of the 8-story building and across Teheran Street (WSW–ENE directed with 11 lanes). A bush fence, with a height of 1 m, is built on the sidewalk with an approximately 5-m distance from the street-side edge of the sidewalk.

During the period of the field experiment, the weather was hot and sunny with occasional showers under the influence of a prevailing high-pressure system. The daytime cloud covers at Seoul meteorological observatory were 0/10–9/10, 6/10–10/10 (shower event), 3/10–7/10, and 2/10–6/10 on 24, 25, 26, and 27 June, respectively. Weak easterly synoptic-scale surface winds were observed on 26 June, but no distinct synoptic-scale surface winds were observed on the other days. In contrast to the synoptic-scale surface winds, somewhat strong westerly sea breezes



Fig. 1. Measurement location indicated over the satellite image (upper left), three-dimensional building map (lower right), and on-site pictures of ultrasonic anemometers and ozone analyzers at the rooftop (A) (upper right) and sidewalk (B) (lower left) sites.

occurred after 1500–1600 LST throughout the whole period. Note that the measurement sites are close to the Yellow Sea (a straight-line distance of ~ 40 km). The sea surface temperature over the Yellow Sea ranged from 17°C to 20°C , and the daytime 2-m air temperature at Gangnam automatic weather station near the measurement sites, which is operated by the Korea Meteorological Administration, rose to as high as 29 – 32°C during the period of the field experiment.

2.2 Instruments

For turbulent flow (wind) measurement, two three-dimensional ultrasonic anemometers (CSAT3, Campbell Scientific) were used. Three orthogonal wind components were measured at a maximum rate of 60 Hz. The two ultrasonic anemometers were installed at a 2-m height above the surfaces with ~ 1 m distance from the 1-m height rooftop wall at the rooftop site (A1, Fig. 1) and with ~ 1 m distance from the 1-m height bush fence at the sidewalk site (B1, Fig. 1). The air temperature was measured using two probes (HM-P155A, Vaisala). The measurement data were processed by measurement and control systems (CR1000, Campbell Scientific) that record wind components data at a 50-Hz rate and air temperature data every minute. All the instruments were powered primarily by portable batteries, with solar panels providing auxiliary power.

Ozone concentrations were measured by UV absorption ozone analyzers at the rooftop (Model 202, 2B Technologies) and sidewalk (T400, Teledyne) sites. These ozone analyzers were placed ~ 1 m above the surfaces at the rooftop (A2, Fig. 1) and sidewalk (B2, Fig. 1) sites. Because the detection limits of the two ozone analyzers are lower than 1 ppb, the ozone analyzers are applicable for exhibiting a diurnal variation of ozone concentration in polluted urban areas. Ozone concentration data measured at the rooftop and sidewalk sites were saved every 5 and 10 minutes, respectively, except for power-off periods because of battery changes or occasional showers.

3. Results and discussion

Figure 2 shows the temporal variations of 30-min averaged air temperature and ozone concentration at the rooftop and sidewalk sites. The time span for air temperature is 72 hours starting from 1500 LST 24 June 2013. The time span for ozone concentration at the rooftop (sidewalk) site is 72 (51) hours starting from 1500 LST 24 (1200 LST 25) June 2013. The air temperature at the sidewalk site is higher than that at the rooftop site. The difference in air temperature between the two sites is larger in the daytime than in the nighttime. The maximum difference in air temperature between the two sites is $\sim 1.4^{\circ}\text{C}$. The ozone concentrations at both sites also show diurnal variations similar to each other. The ozone concentration at the sidewalk site is always lower than that at the rooftop site because of NO_x emission from mobile sources and subsequent NO titration (Xie et al. 2003). The hourly traffic volume manually counted at the sidewalk site is the highest at 0900 LST (~ 4500 vehicles h^{-1}) and remains substantially high from 0800 to 2100 LST over 3000 vehicles h^{-1} on 25 and 26 June. This is a heavy traffic condition resulting in large amounts of NO_x emission on the road. In the daytime, primary and secondary peaks of ozone concentration appear for 1200–1230 LST (115 ppb) and 1630–1700 LST (113 ppb), respectively, on 25 June and for 1330–1400 LST (103 ppb) and 1700–1730 LST (98 ppb), respectively, on 26 June. The earlier peaks are mostly attributed to photochemical production in the urban boundary layer. The later peaks can be attributed to transport by sea breeze from the west (Ryu et al. 2013) as well as photochemical production. The attribution of the later peaks to the sea breeze transport can be inferred by the wind speed and direction measured at the rooftop site. Southerly or easterly wind with wind speeds lower than 2 m s^{-1} is predominant at the time of earlier peaks, whereas southwesterly wind with wind speeds higher than 2 m s^{-1} is predominant at the time of later peaks (see Figs. 3a, b). In the nighttime, a local peak of ozone concentration appears for 0230–0300 LST on 26 June and for 0230–0300 LST on 27 June. Previous studies have

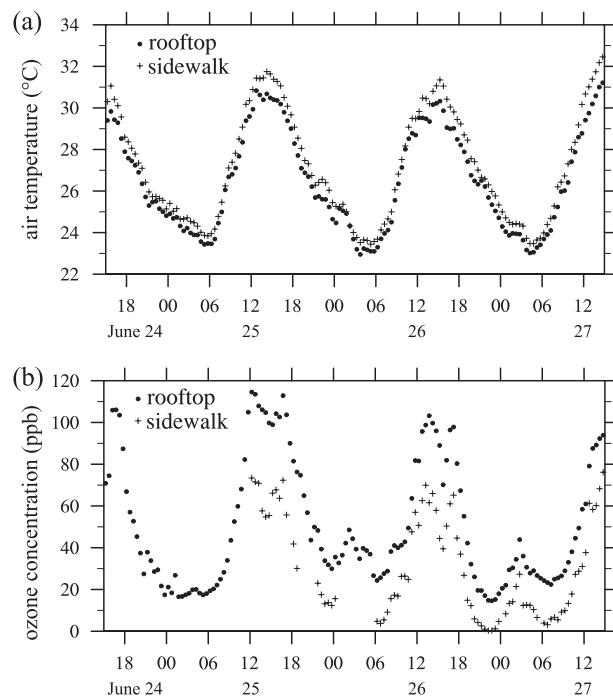


Fig. 2. Temporal variations of 30-min averaged (a) air temperature and (b) ozone concentration at the rooftop and sidewalk sites.

reported that a nighttime peak of ozone concentration appears when low-level jets enhance vertical mixing and hence transport ozone in the residual layer to the surface (Reitebuch et al. 2000; Hu et al. 2013). This possibility in the present study needs to be investigated using a coupled meteorology-air quality model.

The temporal variations of 30-min averaged wind speed, horizontal wind direction, and turbulent kinetic energy (TKE) at both sites for 72 hours starting from 1500 LST 24 June are shown in Fig. 3. For every 30-min averaging period, perturbations of velocity components (u , v , w) from their 30-m averages are squared and averaged to calculate TKE, half the sum of squared and averaged perturbations. Wind speeds at both sites also show diurnal variations similar to each other. This is associated with the development of the atmospheric boundary layer (ABL) in the daytime. Enhanced ABL-mixing in the daytime induces strong wind at the rooftop site (Fig. 3a), but the impact of ABL-mixing does not seem to be significant at the sidewalk site. The maximum 30-m averaged wind speed at the sidewalk is $\sim 1.3 \text{ m s}^{-1}$ (much lower than $\sim 3.7 \text{ m s}^{-1}$ at the rooftop site). In contrast to the temporally varying wind direction at the rooftop site, the wind direction at the sidewalk site is relatively uniform. The wind direction at the sidewalk site is mostly southerly along Nonhyun Street except for several periods (when easterly synoptic-scale surface winds are distinct). The rooftop wind direction is easterly in the early morning, and it becomes westerly in the afternoon after the passage of a sea-breeze front (at ~ 1500 LST). The passage of a sea-breeze front is confirmed in the wind direction, air temperature, and relative humidity measured at Gangnam automatic weather station (not shown). The diurnal variation is also distinct in the time series of TKE at both sites (Fig. 3c). TKE at the rooftop site is mostly higher than that at the sidewalk site because of higher wind speed at the rooftop site. The difference in TKE between the two sites is large for 1500–1800 LST.

Figure 4 shows the multiresolution spectra of horizontal and vertical velocities at the rooftop and sidewalk sites for 2 days starting from 0000 LST 25 June. The multiresolution spectrum analysis enables the decomposition of non-periodic time series, and the fast Haar transform algorithm used for the multiresolution decomposition requires less computation time than the fast Fourier transform (Howell and Mahrt 1997; Vickers and Mahrt 2003).

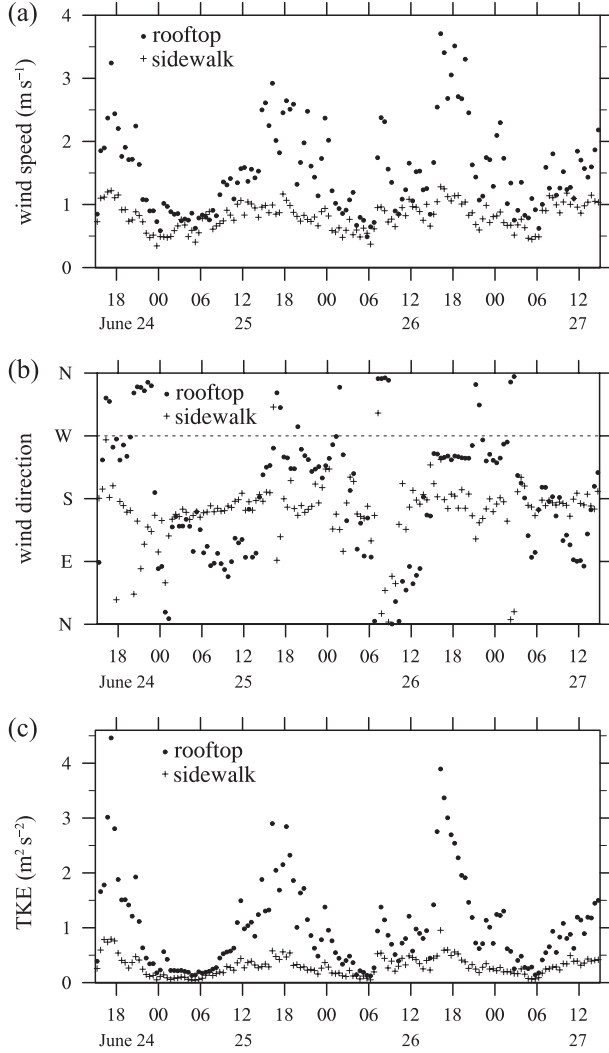


Fig. 3. Temporal variations of 30-min averaged (a) wind speed, (b) horizontal wind direction, and (c) turbulent kinetic energy at the rooftop and sidewalk sites.

First, 50-Hz data for the 2 days are projected on 8388608 (2^{23}) time points. The projected data are binned into 4194304 (2^{22}) bins, and 2-point average and 2-point difference in each bin are calculated. The calculated 2-point averages are used to calculate 4-point averages and 4-point-scale differences, and the same process is repeated until the difference between two 4194304-point averages is calculated. Then, the calculated differences are summed at each averaging time scale, and the sum represents a variation at each time scale. The diurnal (1-day averaging time scale) variation of horizontal velocity is distinct at both sites. A local peak appears at 6-h time scale at the rooftop site. The multiresolution spectrum of horizontal velocity exhibits a turbulence-related local peak at ~ 84 s (~ 42 s) at the rooftop (sidewalk) site. These peaks are similar in time scale to the midfrequency (0.01–0.1 Hz) peaks of premultiplied power spectra within street canyons (Nelson et al. 2007). This similarity indicates that the peaks can be related to turbulence generated by nearby buildings. A spectral gap between turbulence and diurnal (or 6-h) variation appears at both sites. The multiresolution spectrum of vertical velocity at the rooftop site again shows distinct diurnal and 6-h local peaks, but both peaks are absent at the sidewalk site. We speculate that the impacts of local winds (e.g., increased wind speed after the passage of a sea-breeze front) appear as the 6-h local peaks at the rooftop site. The multiresolution spectrum of vertical velocity exhibits a local peak at ~ 5 s at the sidewalk site. This time scale is much smaller than

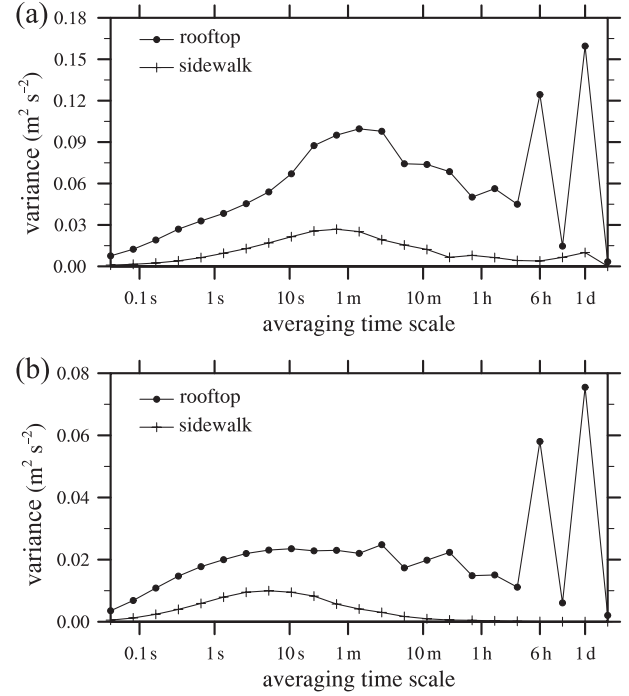


Fig. 4. Multiresolution spectra of (a) horizontal velocity and (b) vertical velocity at the rooftop and sidewalk sites for 2 days starting from 0000 LST 25 June 2013.

that of horizontal velocity. At the rooftop site, the turbulence-related local peak is not distinct.

Figure 5 shows the fields of joint probability density function (PDF) of u' and w' at the rooftop and sidewalk sites for 0800–1400 LST 25 June. Here, u' and w' denote deviations from 30-min averaged streamwise velocity and vertical velocity, respectively. The joint PDF of u' and w' is calculated using the expression (Park et al. 2013),

$$f_{u', w'}(a_i, a_j) = P[a_i - 0.5\Delta a < u' \leq a_i + 0.5\Delta a, a_j - 0.5\Delta a < w' \leq a_j + 0.5\Delta a], \quad (1)$$

where a_i (a_j) and Δa are values of i th (j th) bin and the bin width, respectively. In each direction, 40 bins are used for calculation. The sum of all joint PDFs is one. The vertical turbulent kinematic momentum flux $u'w'$ can be decomposed into four quadrants: outward interaction ($u'_+w'_+$), ejection ($u'_+w'_-$), inward interaction ($u'_-w'_+$), and sweep ($u'_-w'_-$) (Raupach 1981). During a period when westerly wind blows, the rooftop site seems to be significantly affected by the wake behind the upstream high-rise building or by flow structures generated around the west edge of the anemometer-mounted building. Thus, a period of easterly wind (0800–1400 LST 25 June) is selected for the turbulence analysis at both sites. At the rooftop site, frequent ejections and less frequent but stronger sweeps are dominant. This kind of strong-sweep-dominant pattern is attributed to the shear-induced mixing layer near the rooftop surface, and it is similar to patterns over plant canopies (Watanabe 2004) and close to roofs of urban buildings (Christen et al. 2007). Compared to the rooftop site, the distribution of u' and w' at the sidewalk site seems to be less characterizable with smaller u' and w' magnitudes.

4. Summary and conclusions

Short-term measurements of turbulent flow and ozone concentration at the rooftop and sidewalk sites in a high-rise building area of Seoul were performed to examine their characteristics according to site location. Diurnal variations are distinct in the time series of air temperature, wind speed, and TKE at both sites.

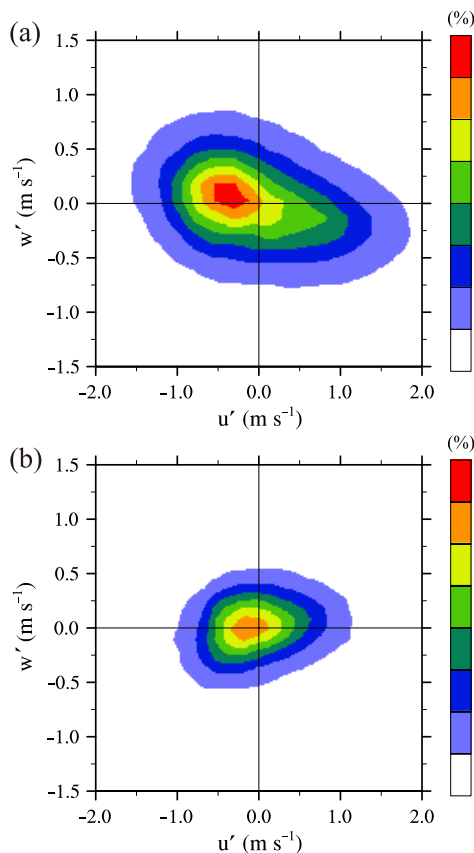


Fig. 5. Fields of joint probability density function of u' and w' at the (a) rooftop and (b) sidewalk sites for 0800–1400 LST 25 June 2013.

The time series of ozone concentration at both sites show diurnal variation with double local peaks in the daytime and one local peak in the nighttime. While the horizontal wind direction at the sidewalk site is mostly southerly along the street, the horizontal wind direction at the rooftop site shows variations related to local winds. Diurnal variations also appear in the multiresolution spectra of horizontal velocity and vertical velocity at the rooftop site, along with turbulence-related variations. The quadrant analysis illustrated that frequent ejections and less frequent but stronger sweeps are dominant at the rooftop site.

Measurements and analyses of turbulent flow and pollutant concentrations in high-rise building areas are an important research subject and can contribute greatly to a better understanding of turbulent flow and dispersion in and above deep street canyons. This study reports turbulence characteristics measured at a rooftop site and a sidewalk site in a high-rise building area of a megacity. Turbulence characteristics can vary depending on weather conditions. Further studies with long-term data are required.

Acknowledgements

The authors are grateful to two anonymous reviewers for providing valuable comments on this work. This work was supported by the National Research Foundation of Korea (NRF) grant funded by the Korea Ministry of Science, ICT and Future Planning (MSIP) (No. 2011-0017041).

References

- Allwine, K. J., J. H. Shinn, G. E. Streit, K. L. Clawson, and M. Brown, 2002: Overview of URBAN 2000: A multiscale field study of dispersion through an urban environment. *Bull. Amer. Meteor. Soc.*, **83**, 521–536.
- Brown, M. J., H. Khalsa, M. Nelson, and D. Boswell, 2004: Street canyon flow patterns in a horizontal plane: Measurements from the Joint URBAN 2003 field experiment. *Extended Abstracts, Fifth Symp. on the Urban Environment*, Vancouver, Canada, Amer. Meteor. Soc., 11 pp.
- Christen, A., E. V. Gersel, and R. Vogt, 2007: Coherent structures in urban roughness sublayer turbulence. *Int. J. Climatol.*, **27**, 1955–1968.
- Howell, J. F., and L. Mahrt, 1997: Multiresolution flux decomposition. *Bound.-Layer Meteor.*, **83**, 117–137.
- Hu, X.-M., P. M. Klein, M. Xue, J. K. Lundquist, F. Zhang, and Y. Qi, 2013: Impact of low-level jets on the nocturnal urban heat island intensity in Oklahoma City. *J. Appl. Meteor. Climatol.*, **52**, 1779–1802.
- Kastner-Klein, P., E. Fedorovich, and M. W. Rotach, 2001: A wind tunnel study of organised and turbulent air motions in urban street canyons. *J. Wind Eng. Ind. Aerodyn.*, **89**, 849–861.
- Letzel, M. O., C. Helmke, E. Ng, X. An, A. Lai, and S. Raasch, 2012: LES case study on pedestrian level ventilation in two neighbourhoods in Hong Kong. *Meteor. Z.*, **21**, 575–589.
- Louka, P., S. E. Belcher, and R. G. Harrison, 2000: Coupling between air flow in streets and the well-developed boundary layer aloft. *Atmos. Environ.*, **34**, 2613–2621.
- Nelson, M. A., E. R. Pardyjak, M. J. Brown, and J. C. Klewicki, 2007: Properties of the wind field within the Oklahoma City Park Avenue street canyon. Part II: Spectra, cospectra, and quadrant analyses. *J. Appl. Meteor. Climatol.*, **46**, 2055–2073.
- Nelson, M. A., E. R. Pardyjak, and P. Klein, 2011: Momentum and turbulent kinetic energy budgets within the Park Avenue street canyon during the Joint Urban 2003 field campaign. *Bound.-Layer Meteor.*, **140**, 143–162.
- Park, S.-B., J.-J. Baik, and B.-S. Han, 2013: Large-eddy simulation of turbulent flow in a densely built-up urban area. *Environ. Fluid Mech.*, doi:10.1007/s10652-013-9306-3.
- Princevac, M., J.-J. Baik, X. Li, H. Pan, and S.-B. Park, 2010: Lateral channeling within rectangular arrays of cubical obstacles. *J. Wind Eng. Ind. Aerodyn.*, **98**, 377–385.
- Raupach, M. R., 1981: Conditional statistics of Reynolds stress in rough-wall and smooth-wall turbulent boundary layers. *J. Fluid Mech.*, **108**, 363–382.
- Reitebuch, O., A. Strassburger, S. Emeis, and W. Kuttler, 2000: Nocturnal secondary ozone concentration maxima analysed by sodar observations and surface measurements. *Atmos. Environ.*, **34**, 4315–4329.
- Rotach, M. W., 1995: Profiles of turbulence statistics in and above an urban street canyon. *Atmos. Environ.*, **29**, 1473–1486.
- Roth, M., and T. R. Oke, 1993: Turbulent transfer relationships over an urban surface. I: Spectral characteristics. *Quart. J. Roy. Meteor. Soc.*, **119**, 1071–1104.
- Ryu, Y.-H., J.-J. Baik, K.-H. Kwak, S. Kim, and N. Moon, 2013: Impacts of urban land-surface forcing on ozone air quality in the Seoul metropolitan area. *Atmos. Chem. Phys.*, **13**, 2177–2194.
- Vickers, D., and L. Mahrt, 2003: The cospectral gap and turbulent flux calculations. *J. Atmos. Oceanic Technol.*, **20**, 660–672.
- Watanabe, T., 2004: Large-eddy simulation of coherent turbulence structures associated with scalar ramps over plant canopies. *Bound.-Layer Meteor.*, **112**, 307–341.
- Wood, C. R., and Coauthors, 2009: Dispersion experiments in central London: The 2007 DAPPLE project. *Bull. Amer. Meteor. Soc.*, **90**, 955–969.
- Xie, S., Y. Zhang, L. Qi, and X. Tang, 2003: Spatial distribution of traffic-related pollutant concentrations in street canyons. *Atmos. Environ.*, **37**, 3213–3224.
- Zajic, D., H. J. S. Fernando, R. Calhoun, M. Princevac, M. J. Brown, and E. R. Pardyjak, 2011: Flow and turbulence in an urban canyon. *J. Appl. Meteor. Climatol.*, **50**, 203–223.